Biosensors and Bioelectronics 28 (2011) 166–173

Contents lists available at ScienceDirect

Biosensors and Bioelectronics

journal homepage: www.elsevier.com/locate/bios

Polyaniline protected gold nanoparticles based mediator and label free electrochemical cortisol biosensor

Sunil K. Arya*, Abhishek Dey, Shekhar Bhansali*

Bio-MEMS and Microsystem Lab, Department of Electrical Engineering, University of South Florida, Tampa, FL 33620, United States

ARTICLE INFO

Article history:
Received 19 May 2011
Received in revised form 6 July 2011
Accepted 8 July 2011
Available online 20 July 2011

Keywords:
Cortisol
Polyaniline
Cyclic voltammetry
Biosensor
Gold nanoparticles

ABSTRACT

Polyaniline protected gold nanoparticles (PPAuNPs) were electrophoretically deposited onto a gold electrode, and utilized to fabricate an electrochemical cortisol biosensor. Cortisol specific monoclonal antibody (C-Mab) was covalently immobilized onto the surface of a PPAuNP/Au electrode using N-ethyl-N′-(3-dimethylaminopropyl) carbodiimide and N-hydroxysuccinimide (EDC/NHS) chemistry. BSA was employed for blocking nonspecific adsorption on the electrode surface. PPAuNP formation and BSA/C-Mab/PPAuNP/Au electrode fabrication were characterized using transmission electron microscopy, atomic force microscopy and electrochemical impedance techniques, respectively. Cyclic voltammetry and differential pulse voltammetric techniques were used to determine the cortisol concentration in a phosphate buffer saline (PBS) solution. Results confirmed that the PPAuNP based electrode was stable during repeated scans and exhibited repeatable redox peaks. Further, the BSA/C-Mab/PPAuNP/Au electrode in the PBS buffer accurately detected cortisol in the range of 1 pM–100 nM with a sensitivity of 1.63 $\mu A\,M^{-1}$. The biosensor was found to be selective against BSA and 17-α-hydroxy progesterone. This research establishes the feasibility of using a PPAuNP based matrix for a label and mediator free electrochemical biosensor for cortisol, a stress biomarker.

1. Introduction

Electrochemical biosensors have shown potential for fast, accurate and sensitive health care monitoring at a patient's bedside (Wang, 2006). However, a continuing challenge in the wider use of biosensors has been the sensitivity and stability of the surface bound biosensing molecules. The sensitivity and selectivity is crucially dependent on the matrix used for their immobilization in the sensor. The biosensing molecules need to be integrated with a redox active system in a bio-compatible environment to obtain an optimum output from the electrochemical biosensor. In electrochemical biosensors, conducting polymers and their composites have attracted much interest as suitable matrices for biomolecule binding, enhanced stability, speed, and sensitivity (Koh et al., 2010; Malhotra et al., 2006; Wang et al., 2011). Polyaniline (PANI) has been one such material of interest. PANI's conducting properties, stability, ease of electron transfer and ease of synthesis are key features that make it attractive for its use in electrochemical biosensing (Dhand et al., 2011). It possesses a large number of amino groups that can be used for easy binding of biosensing molecules. Additionally, improvement in redox stability and electro-activity of PANI based composite systems during electrochemical analysis in neutral pH environment has triggered its use in composite form: with carbon nanotubes (CNTs), gold nanoparticles (AuNPs), and other materials (Dhand et al., 2008a,b; Feng et al., 2006; Gajendran and Saraswathi, 2008; Spain et al., 2011; Tian et al., 2004). The presence of nanomaterials such as AuNP in the composite results in large surface area to volume ratio with PANI providing the functional groups, thus nanocomposite providing increased surface area (and functional groups) result in improved sensitivity.

Dhand et al. described the fabrication of a PANI–CNT composite for biosensor applications (Dhand et al., 2008b). They observed that the presence of CNTs in the matrix acts as the dopant for PANI, and stabilizes the system during electrochemical measurements. It was observed that this led to a steady and reversible behavior in the composite. Feng et al. investigated a PANI–AuNP matrix based electrochemical DNA biosensor, and showed that the use of this composite resulted in enhanced immobilization of the DNA probe and detection sensitivity of the target DNA (Feng et al., 2008). In another study, Ozdemir et al. described a pyranose oxidase modified AuNP–PANI/AgCl hybrid nanocomposite matrix based glucose biosensor. They stated that the use of a nanocomposite matrix improved the bioactivity and stability of the bound enzyme in operational conditions (Ozdemir et al., 2010). Liu et al. demonstrated a highly electro-active polystyrene–PANI–Au composite

* Corresponding authors. Tel.: +1 8139743593.
E-mail addresses: sunilarya333@gmail.com (S.K. Arya), sbhansali@gmail.com (S. Bhansali).

0956-5663/$ – see front matter © 2011 Elsevier B.V. All rights reserved.
doi:10.1016/j.bios.2011.07.015

based glucose biosensor. They showed that the composite exhibited improved electrical conductivity and showed a well-defined redox peak and high catalytic activity for the enzyme bound electrode (Liu et al., 2008). In all of these composite formations, composite components were prepared separately and then blended with each other by different processing techniques. Recently, tetrachloroaurate (III) ($AuCl_4^-$) ions have been reported to act as an oxidant in the oxidative polymerization of pyrrole and aniline to form gold nanostructures capped with their polymers (Njagi and Andreescu, 2007; Shiigi et al., 2009, 2006; Wang et al., 2005). This results in formation of a uniform composite in a single step and hence reduces the steps required for electrode fabrication. Yang et al. described PANI–Au composite formation via oxidative polymerization of aniline, using $HAuCl_4$ as the oxidant and 1-butyl-3-methylimidazolium hexafluorophosphate as the growth media. They observed that an electrode fabricated using a composite possesses high conductivity, a large specific surface area, and excellent electro-activity, and thus can serve as an excellent matrix for enzyme immobilization and electrocatalysis (Yang et al., 2008). In the present work, PPAuNPs have been successfully prepared in a single step using $HAuCl_4$ as the oxidant and HCl as the growth media.

Uniform deposition of the preformed polymer on a suitable sensor surface has been another major challenge in biosensor fabrication. Though techniques such as drop casting and spin casting are easy and can be used for producing films from preformed polymers, deposition of preformed polymers and nanostructures using an electrophoretic deposition (EPD) technique has shown promise for yielding uniform and dense films (Dhand and Malhotra, 2009; Dhand et al., 2007; Murphy-Perez et al., 2011). EPD is a simple and cost-effective technique, amenable to scaling-up to large dimensions, and applicable to a great variety of materials. In EPD, charged molecules dispersed in a suitable solvent move towards an electrode of opposite polarity, and get deposited as homogeneous and highly dense films via particle coagulation (Dhand and Malhotra, 2009). The deposition of uniform and smooth films of PANI and PANI–multi-wall CNT films on an indium-tin-oxide (ITO) coated glass plate using EPD was described recently (Dhand et al., 2008b, 2007). Li et al. demonstrated the electrophoretic deposition of chitosan–hemoglobin film, and showed that film composition and deposition yield can be controlled (Li et al., 2011). Using laccase modified, EPD deposited mesoporous silica powder onto a glassy carbon electrode, Shimomura et al. described the fabrication of a catechol biosensor. Results suggested improved detection in the 2–100 μM range, with a response time of approximately 2 min (Shimomura et al., 2011).

This paper presents our results on the use of PPAuNPs for cortisol detection. There has been growing interest in the measurement of cortisol, a potential biomarker for Post-Traumatic Stress Disorder (PTSD) (Hauer et al., 2009). Cortisol, a steroid hormone, is an important molecule for the regulation of blood pressure, glucose levels and carbohydrate metabolism (Stevens et al., 2008; Tai and Welch, 2004; Zhou et al., 2004). Its periodic estimation is required, as an abnormal increase can cause the development of Cushing's disease, inflammation and a depressed immune system, while decreased levels can lead to Addison's disease (Stevens et al., 2008; Zhou et al., 2004). Currently, in clinical practice, cortisol is measured using either traditional lab based techniques, such as high performance liquid chromatography (HPLC), fluorometric assay, and reverse phase chromatography, or via alternate techniques, such as radioimmunoassay (RIA), flow immunoassay and enzyme-linked immunosorbent assay (ELISA) (Appel et al., 2005; Cook et al., 1997; Gatti et al., 2005; Kaptein et al., 1997; Koutny et al., 1996; Oka et al., 1987; Sarkar et al., 2007; Schmalzing et al., 1995; Zhou et al., 2004). Though these techniques are sensitive, they have their limitations and cannot be implemented at the point of care. Recently, various biosensors have been reported for easy cortisol estimation (Arya et al., 2010a,b; Kumar et al., 2007; Mitchell et al., 2009; Stevens et al., 2008; Sun et al., 2008; Zhou et al., 2004), however, these biosensors involve mediators, multi step electrode fabrication, indirect cortisol estimation, measurement at high voltages, and/or modification of the analyte itself.

In this work, we report a successful fabrication of a label and mediator free electrochemical biosensor for ultrasensitive cortisol testing. This work demonstrates that conducting polymer composite (PANI protected AuNPs (PPAuNPs)) after electrophoretic deposition on a gold surface can be used as a matrix for label and external mediator free electrochemical biosensor fabrication. For selective cortisol estimation, cortisol antibody (C-Mab) was immobilized using N-ethyl-N′-(3-dimethylaminopropyl) carbodiimide and N-hydroxysuccinimide (EDC/NHS) chemistry onto a PPAuNPs/Au electrode, and nonspecific binding was prevented via BSA blocking. The sensor was tested for cortisol estimation in a phosphate buffer saline (PBS) solution using cyclic voltammetry, and was found to detect cortisol up to 1 pM with a sensitivity of 1.63 $\mu A\,M^{-1}$.

2. Materials and methods

2.1. Chemicals and reagents

The aniline, hydrogen tetrachloroaurate (III) trihydrate, EDC, NHS and hydrocortisone (cortisol) were purchased from Sigma Aldrich. The monoclonal cortisol antibody (anti-cortisol, C-Mab) 2330-4809 was procured from Abd serotec. All other chemicals were of analytical grade and were used without further purification. The working solutions of hydrocortisone were prepared by dilution in PBS (10 mM, pH 7.0, 0.9% NaCl).

2.2. Synthesis of polyaniline protected gold nanoparticles (PPAuNPs)

PPAuNP synthesis was carried out using aniline as a precursor and $HAuCl_4$ as the oxidant. For synthesis, a 0.1 M aniline solution was prepared in 10 ml of 0.1 N aqueous HCl solution via sonication, and then stirred at 300 rpm using a magnetic stirrer. To this, 1 mM $HAuCl_4$ solution in deionized water (18.2 MΩ) was added dropwise and the resulting mixture was stirred for another 30 min. As the reaction proceeded, the solution color changed from yellow to blue, and finally to dark green. After synthesis, the solution was centrifuged to collect the PPAuNP precipitate and the supernatant was discarded. The precipitate was washed three times via resuspension in 3 ml of water using sonication followed by centrifugation. Finally, the precipitate was resuspended in 1 ml of water and stored until further use (Fig. 1). This procedure resulted in the formation of a nanocomposite with uniform composition in a single step.

2.3. Electrophoretic deposition (EPD) of PPAuNPs onto a gold electrode

For EPD, PPAuNPs resuspended in 1 ml of water was mixed with 24 ml of formic acid and sonicated for 30 min to make the stock solution. 200 μl of this stock solution was added to 1.8 ml of acetonitrile, and sonicated for 1 min to prepare the colloidal deposition solution. Gold electrodes (2.5 cm × 0.5 cm) were prepared via chrome/gold (10 nm/100 nm) deposition on thermally oxidized 4 inch. Si wafers, using e-beam evaporation followed by dicing. PPAuNP films using a prepared colloidal solution were deposited electrophoretically onto an Au surface (0.5 cm × 0.5 cm). Deposition was carried out in a two-electrode cell configuration, with gold foil (10 mm × 30 mm) as the counter electrode and a pre-cleaned Au substrate as the working electrode. The two electrodes were placed parallel to each other with a separation of 5 mm, and dipped

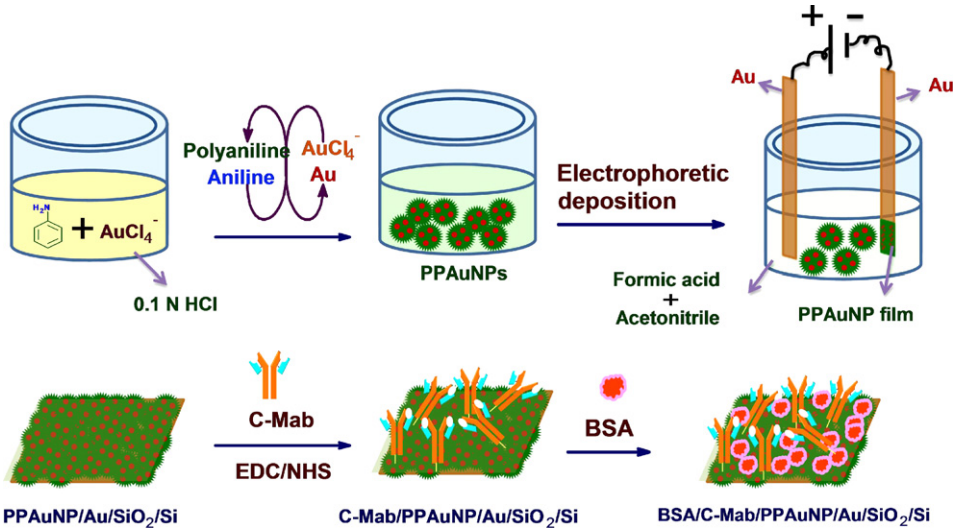

Fig. 1. Schematic for BSA/C-Mab/PPAuNP/Au electrode fabrication.

in the PPAuNP working colloidal suspension. Film deposition time and voltage were optimized, and a stable response was observed for the films (25 mm^2) deposited at 60 V for about 60 s. The films were then removed from the suspension, washed with deionized water and dried in air (Fig. 1). The deposition resulted in repeatable, strongly adhered and uniform films. The thickness of the deposited films was measured using a Dektak surface profiler and found to be around 250 nm.

2.4. Covalent binding of C-Mab onto a PPAuNP/Au electrode

Covalent immobilization of C-Mab was achieved via amide bond formation between an NH_2 group of PANI and a COOH group of C-Mab, using EDC as the coupling agent and NHS as the activator. For binding, 30 μl of 2 μg ml^{-1} C-Mab solution in PBS (10 mM, pH 7.0, 0.9% NaCl) containing 0.4 M EDC and 0.1 M NHS was poured onto the PPAuNP/Au electrode (25 mm^2 area) and incubated for 90 min in a humid chamber. The fabricated C-Mab/PPAuNP/Au electrode was washed with PBS (10 mM, pH 7.0) containing 0.9% NaCl and 0.05% Tween 20 to remove any unbound C-Mab, followed by 30 min of incubation in a 10 μg ml^{-1} BSA solution in PBS (10 mM, pH 7.0, 0.9% NaCl) for blocking of nonspecific binding. The fabricated BSA/C-Mab/PPAuNP/Au electrode was washed and stored at 4 °C when not in use (Fig. 1). Electrochemical characterization revealed a maximum variation of ±3% in the current between the BSA/C-Mab/PPAuNP/Au electrodes prepared in same batch, thus indicating repeatability of the fabrication procedure. Fig. 1 shows the schematic for PPAuNP preparation, deposition and modification of the gold substrate with C-Mab and BSA.

2.5. Characterization

Synthesis of PPAuNPs and their electrophoretic deposition were confirmed by transmission electron microscopy (TEM) measurements using an FEI Tecnai™ TEM, and atomic force microscope (AFM) measurements using a Digital Instrument Nanoscope, respectively. TEM sample was prepared by dipping the Cu grid in PPAuNP/H_2O solution followed by drying in air. Electrochemical impedance (EIS) characterization for electrode fabrication, and voltammetric studies via cyclic voltammetric (CV) and differential pulse voltammetry (DPV) studies for cortisol estimation were carried out in a 5 ml three-electrode cell using an Autolab Potentiostat/Galvanostat (Eco Chemie, Netherlands). In the cell, Ag/AgCl was used as reference electrode and gold as counter electrode. Ag/AgCl reference electrode was made in-house by coating 90:10::Ag:AgCl paste over an Ag wire, followed by drying at 150 °C for 2 h. EIS studies were carried out in a PBS solution (10 mM, pH 7.0, 0.9% NaCl) containing a mixture of 5 mM $Fe(CN)_6^{4-}$ (ferrocyanide), and 5 mM of $Fe(CN)_6^{3-}$ (ferricyanide) i.e. 5 mM $Fe(CN)_6^{3-/4-}$ as a redox probe, at equilibrium potential, without external biasing, in the frequency range of 0.1–10^5 Hz with 10 mV amplitude. CV and DPV studies were carried out in the range of −0.6 V to 0.6 V in 5 ml of PBS (10 mM, pH 7.0, 0.9% NaCl).

3. Results and discussion

3.1. TEM and AFM studies

The TEM image of the as-prepared PPAuNPs (Fig. 2(a)) indicates the formation of spherical PPAuNP composite structures of about 7–15 nm size. The EDAX analysis confirms the presence of gold, carbon and nitrogen (Fig. 2(b)) in the prepared nanocomposite. The peak of copper in Fig. 2(b) is attributed to the copper grid used as a carrier for the samples.

Fig. 2(c) and (d) shows the AFM image of PPAuNP/Au electrode and the BSA/C-Mab/PPAuNP/Au electrode, respectively. From Fig. 2(c), it is clear that the PPAuNP/Au electrode surface has a dense and uniform morphology. Surface roughness analysis (Supplement Fig. 1(a)) reveals a roughness of ∼5.3 nm. However, after BSA and C-Mab binding, the surface becomes rougher and exhibits globular morphology (Fig. 2(d)). The increase in roughness for BSA/C-Mab/PPAuNP/Au surface to around 29 nm (Supplement Fig. 1(b)), and presence of globular structures indicate the binding of antibody and BSA. Change of 100 nm in scale is attributed to the presence of stray structures at certain places on the surface. Such large structures in certain areas can be attributed to the binding chemistry used involving EDC and NHS, which can result in some inter molecular binding between various antibodies along with binding on PPAuNP surface.

3.2. Electrochemical impedance (EIS) studies

EIS studies were used to characterize and record charge transfer processes occurring at the electrode–solution or modified electrode–solution interfaces. EIS studies are well established and known for characterization of an electrode–solution interface. Any change in the EIS spectra can be related to the change in interface properties, thus can be utilized for surface modification character-

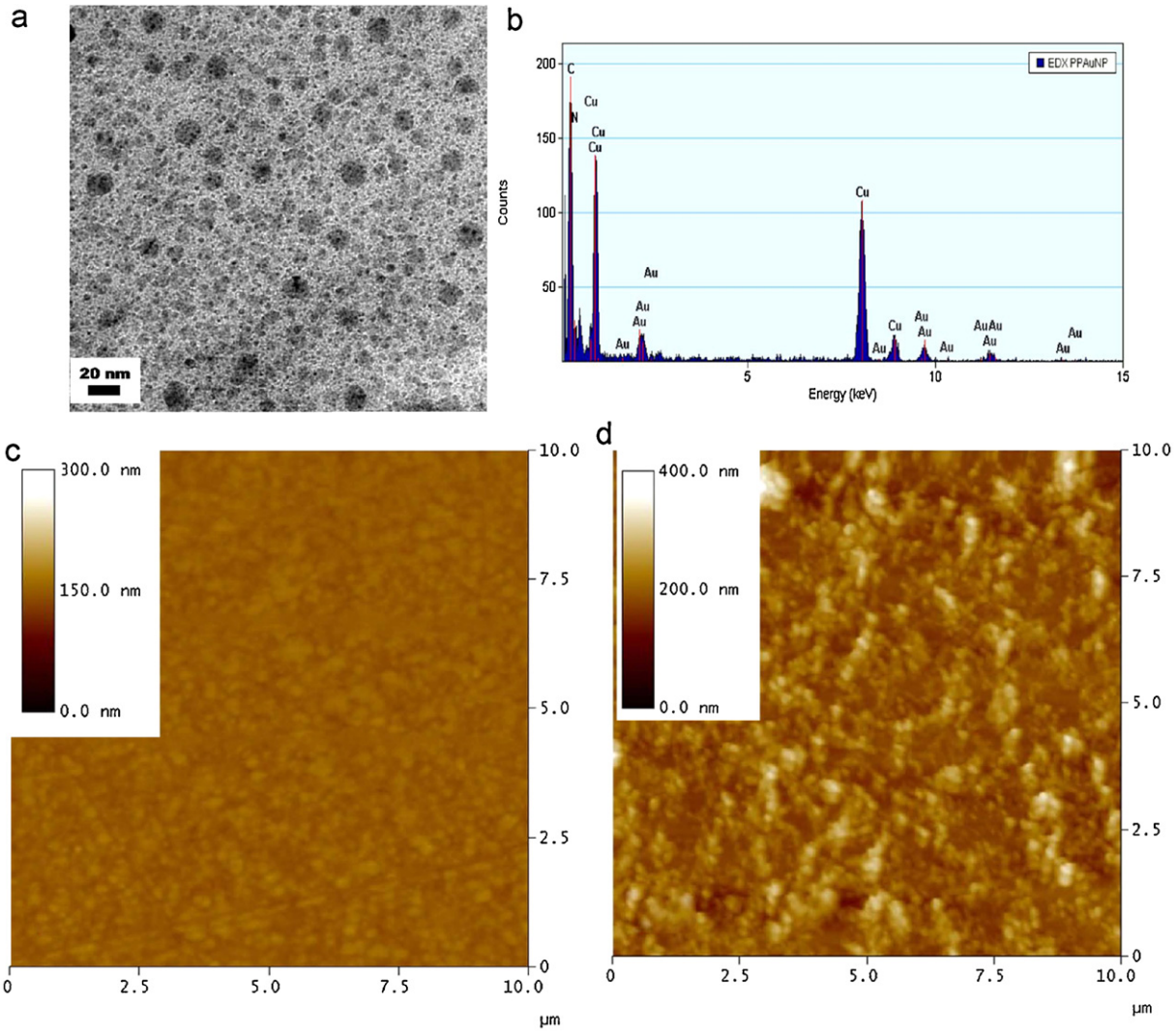

Fig. 2. (a) TEM image of PPAuNPs, (b) EDAX spectra of PPAuNPs, (c) AFM image of the PPAuNP/Au electrode and (d) AFM image of the BSA/C-Mab/PPAuNP/Au electrode.

ization. In the present study, Nyquist plots of impedance spectra were found to be the same for repeated scans of a particular surface, and found to change only after each step of modification. Thus, for characterization of surface modification using charge transfer resistance (R_{ct}), Nyquist plots of impedance spectra were used in the present study.

In Nyquist spectra, magnitude of the R_{ct} (semicircle diameter) depends on the dielectric and insulating features at the electrode–electrolyte interface and can reveal electrode–electrolyte interface properties. Fig. 3 shows the Nyquist plots in a PBS solution (10 mM, pH 7.0, 0.9% NaCl) containing 5 mM $Fe(CN)_6^{3-/4-}$ for various steps in BSA/C-Mab/PPAuNP/Au electrode fabrication. The inset in Fig. 3 shows the Nyquist plot for a blank gold surface and the corresponding equivalent circuit. The Z' (real part of impedance) value at the start of the curve, and the Z' value covered between the semicircular part represent the values of R_s and R_p, respectively, in circuit. Further, the formation of a semicircle and presence of linearly increasing points at the lower frequency region of the curve are attributed to the CPE (constant phase element) and W (warburg impedance), respectively. In curve (ii) of Fig. 3, the increase in R_{ct} from 39 Ω for Au electrode to 590 Ω indicates the buildup of PPAuNP film on the Au surface after electrophoretic deposition. The increase in R_{ct} from 590 Ω

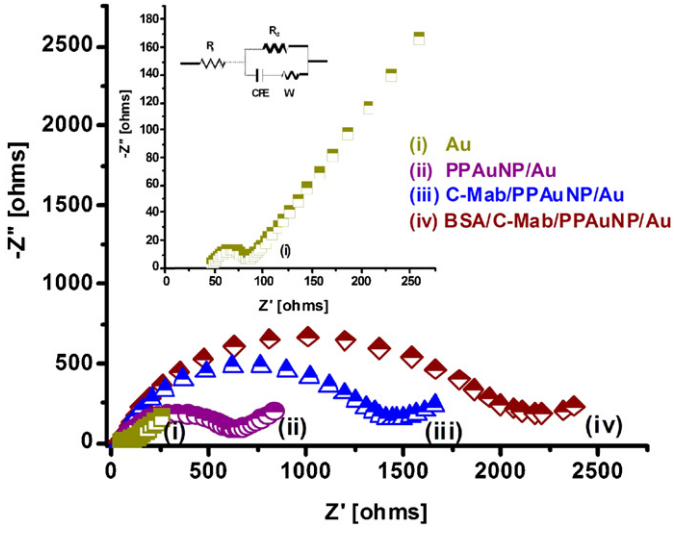

Fig. 3. Nyquist spectra for (i) Au, (ii) PPAuNP/Au electrode, (iii) C-Mab/PPAuNP/Au electrode and (iv) BSA/C-Mab/PPAuNP/Au electrode. *Inset*: Nyquist spectra for Au and the corresponding equivalent circuit.

to 1304 Ω after antibody coupling in curve (iii) is attributed to the binding of the antibodies. The increase is attributed to the insulating nature of the antibodies that reduces the transfer of the charge from the solution to electrode surface. Further, in curve (iv), the increase in R_{ct} to 1867 Ω after BSA incubation indicates the blocking of free spaces (spaces where the antibodies did not bind) on the electrode with BSA protein molecules.

3.3. Cyclic voltammetry (CV) studies

CV is a common electrochemical technique used for determining the electro-active behavior of materials. In the present study, CV has been used to investigate the electro-active behavior of the PPAuNP/Au electrode and the BSA/C-Mab/PPAuNP/Au electrode. Pure PANI is known to exhibit electro-activity at an acidic pH; however, in composite form with metal particles, it is known to exhibit electro-activity even at a neutral pH (Liu et al., 2008).

In the present study, PPAuNP based electrodes were found to be stable during repeated scans and showed no degradation with scanning. Further, the observance of prominent and stable redox peaks, even in the absence of an external mediator, suggested that the material is electrochemically active and can act as a good matrix in the fabrication of a mediator free electrochemical system. Moreover, different PPAuNP/Au electrodes or BSA/C-Mab/PPAuNP/Au electrodes prepared in the same batch were found to exhibit similar current value with maximum variation of ±1.5% and ±3%, respectively. For concentration studies, a new electrode was used for each concentration, and for BSA/C-Mab/PPAuNP/Au calibration, each concentration was the tested using at least three electrodes and the results were plotted in a graph.

3.3.1. Scan rate studies for PPAuNP/Au electrodes and BSA/C-Mab/PPAuNP/Au electrodes

Fig. 4(a) shows the CV studies of the PPAuNP/Au electrode in a PBS solution (10 mM, pH 7.0, 0.9% NaCl) at different scan rates, ranging from 10 to 100 mV s^{-1}. It is clear from Fig. 4(a) that the magnitude of current response increases with an increasing scan rate, exhibiting an almost linear relationship, and follows I (μA) = 13.87 + 1.02ν (mV s^{-1}) (inset of Fig. 4(a)). The slight variation from linearity is attributed to the fact that PPAuNP is not an ideal redox molecule and loses some electrons during the oxidation–reduction cycle, and in transport via the polymer matrix. However, approximate linearity for the increase in peak current with an increasing scan rate, and well defined redox peaks indicate a surface controlled process. The separation of peaks suggests that the process is not perfectly reversible; however, stable redox peak current and position during repeated scans at a particular scan rate suggest that composite based electrodes exhibit a quasi-reversible process.

Fig. 4(b) shows the scan rate response for the BSA/C-Mab/PPAuNP/Au electrode. It can be seen that after binding of C-Mab and BSA on the PPAuNP/Au electrode, the oxidation current and redox peak potential decrease. The decrease in current suggests the binding of BSA and C-Mab and is attributed to the insulating nature of BSA and C-Mab, thus reducing the peak current for the BSA/C-Mab/PPAuNP/Au electrode. Similar to the PPAuNP/Au electrode, linear behavior between the magnitude of the anodic current response and the scan rate following I (μA) = 10.19 + 0.96ν (mV s^{-1}) (inset of Fig. 4(b)), suggests a thin layer electrochemistry with a surface controlled electrochemical process for the BSA/C-Mab/PPAuNP/Au electrode. In both the PPAuNP/Au electrode and the BSA/C-Mab/PPAuNP/Au electrode, CV shows prominent redox peaks in PBS and is stable during repeated scanning. Further, the redox peak difference is minimal and the potential is low enough to avoid possible interference from biological samples. Thus, use of the PPAuNP/Au electrode is advantageous for matrix application in

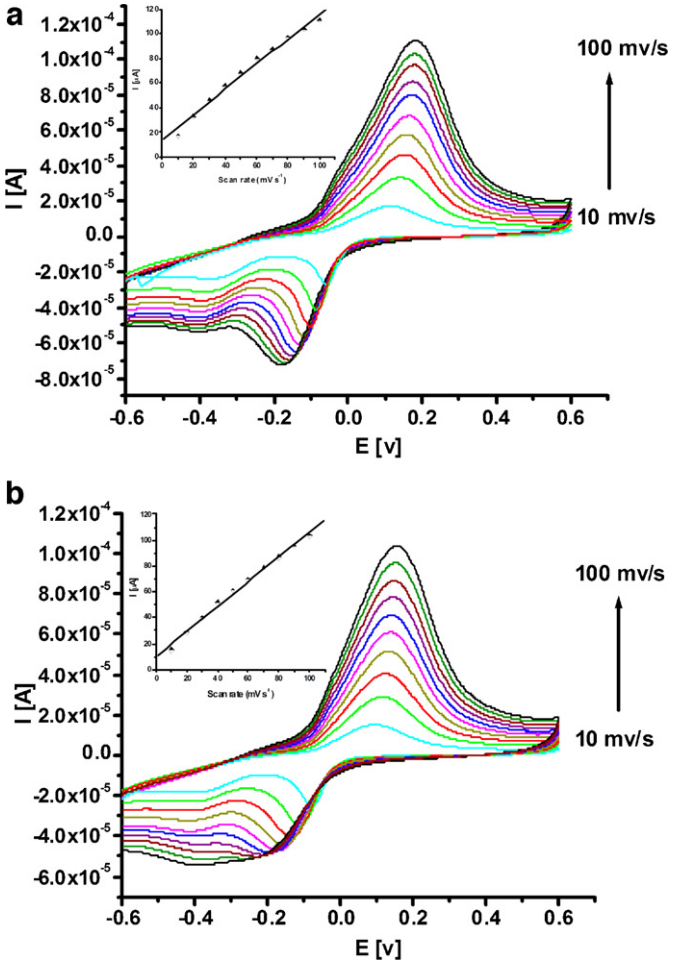

Fig. 4. Scan rate studies for (a) PPAuNP/Au electrode and (b) BSA/C-Mab/PPAuNP/Au electrode.

mediator free biosensors. On analysis, it was found that at a scan rate of 30 mV s^{-1}, the electrode exhibits a stable and equal oxidation and reduction peak area and current values. Thus, all further CV studies were carried out at a scan rate of 30 mV s^{-1}.

The surface concentration of electro-active species (Γ^*) (Rui et al., 2010; Sun et al., 2009) using Faraday law $Q = nFA\Gamma^*$ (where F is the Faraday constant, Q is obtained by integrating an anodic peak, A is the area of the electrode, and n is the number of electrons transferred (2) (Singh et al., 2010)) for the PPAuNP/Au electrode and the BSA/C-Mab/PPAuNP/Au electrode was found to be 1.03×10^{-8} and 8.88×10^{-9} mol cm^{-2}, respectively, at a scan rate of 30 mV s^{-1}. The decrease in the value of Γ^* for the BSA/C-Mab/PPAuNP/Au electrode is attributed to the blocking of the electro-active species by the immobilized BSA and C-Mab.

3.3.2. pH studies

Binding of proteins may result in rearrangement and conformational changes in their structures (Pandey et al., 2007). Such changes can result in the change of their optimum activity at a particular pH value. The ability of amino acids present at the active sites of the antibody to interact with antigen depends on their electrostatic state and conformation, which in turn depends on the pH of the solution. Dependence of antibody activity on their conformation, and thus on pH, makes pH study important in immunosensor fabrication.

To investigate the optimal pH for cortisol estimation, the activity of the BSA/C-Mab/PPAuNP/Au electrode was investigated in the pH range of 6.0–8.0 at room temperature. The effect of pH on the CV

Table 1
Comparison of the BSA/C-Mab/PPAuNP/Au electrode with the electrodes reported in the literature for the cortisol estimation.

Matrix	Sensing molecule	Analyte	Transducer	Secondary label	Mediator/target	pH	Incubation time	Linear range	Ref.
TMOS sol–gel monoliths	Anti-cortisol	Cortisol	Fluorescence	OG-cortisol	n/a	7.2	3 h	1–100 μg ml^{-1}	Zhou et al. (2004)
BSA blocked microtiter plate well	Anti-cortisol	Cortisol	Luminescence	Aequorin-cortisol	n/a	7.5	30 min	1×10^{-5}–1×10^{-9} M	Rowe et al. (2007)
BSA–Anti-rabbit IgG/microtiter plate	Cortisol specific antiserum	Cortisol	EIA	Cortisol-HRP	TMB with urea hydrogen peroxide	7.2	Overnight	0.4–100 pg/well	Sarkar et al. (2007)
Compound 6/CM5 dextran chip	Cortisol derivative	Cortisol	SPR	Anti-cortisol + IgG-HRP	n/a	–	15 min	Up to 49 pg ml^{-1}	Mitchell et al. (2009)
DTSP/Au	Anti-cortisol	Cortisol	EIS	n/a	$Fe(CN)_6^{3-/4-}$	7.4	30 min	1 pM–10 nM	Arya et al. (2010a)
Casein/cortisol–BSA/Au	Anti-cortisol	Cortisol	SPR	n/a	n/a	–	10 min	Up to 1 nM	Stevens et al. (2008)
Streptavidin/paramagnetic particles in solution	Anti-cortisol	FITC-cortisol	Fluorescence	n/a	n/a	7.4	3 h	300 pM–30 nM	Petkus et al. (2006)
Thiotic acid/Au	Anti-cortisol	Cortisol	CV	AP-anti-cortisol	pNPP	9.8	45 min	1 fM–1 mM	Sun et al. (2008)
PPAuNP/Au	Anti-cortisol	Cortisol	CV	n/a	n/a	7.0	30 min	1 pM–100 nM	Present work

TMOS, tetramethylorthosilicate; OG-cortisol, ogregon green conjugated cortisol; EIA, enzyme immunoassay; HRP, horseradish peroxidase; TMB, 3,3′,5,5′-tetramethyl benzidene; SPR, surface plasmon resonance; compound 6, (13-amino-4,7,10-trioxatridecanyl)-3-(11β,17α,21-trihydroxypregn-4-ene-3,20-dione-4-yl)thiopropanimide; DTSP, dithiobis succinimidyl propionate; FITC, fluorescein isothiocyanate labeled cortisol; AP, alkaline phosphatase; pNPP, p-nitrophenyl phosphate; AuNW, gold nanowire; SWV, square wave voltammetry; n/a, not applicable.

response of the BSA/C-Mab/PPAuNP/Au electrode was studied in PBS (10 mM, 0.9% NaCl) (Supplement Fig. 2). It was observed that the peak current and potential vary with the value of pH in the range of 6.0–8.0, and the maximum current was observed in the pH 6.0–7.0 range. We postulate that this is due to the doping effect of PANI in acidic solution. However, the most stable response with equal oxidation and reduction peak area and current was observed for pH 7.0. Further, with the increase of pH, the oxidation potential shifted linearly to the negative side of potential with a slope of 44.7 mV pH^{-1}. For a perfectly reversible proton coupled electron transfer process, the slope should be 59 mV pH^{-1}, however, the BSA/C-Mab/PPAuNP/Au electrode did not show perfectly reversible behavior; thus, the obtained value was less than 59 mV pH^{-1}. For cortisol concentration studies at pH 6.0 (Supplement Fig. 3), no activity was observed. The absence of activity at pH 6.0 can be attributed to the low affinity of C-Mab for cortisol at an acidic pH. Thus, due to physiological conditions and the stable response at pH 7.0, all concentration studies were performed at pH 7.0.

3.3.3. *Cortisol response studies of the BSA/C-Mab/PPAuNP/Au electrode*

To study the activity of the BSA/C-Mab/PPAuNP/Au electrode, CV experiments at a scan rate of 30 mV s^{-1} were conducted after incubation of the electrode for 30 min in a PBS (10 mM, pH 7.0, 0.9% NaCl) solution containing a specific cortisol concentration. Different BSA/C-Mab/PPAuNP/Au electrodes prepared in the same batch were found to exhibit similar current value with maximum variation of ±3%; thus for each concentration, a new electrode was used. For calibration, each concentration was tested using at least three electrodes and a graph was plotted (Fig. 5).

Incubation resulted in binding of the antigen on the immobilized antibody, thus making the electrode more insulating with an increasing concentration of cortisol. The insulating behavior of cortisol binding was investigated by recording the decrease in peak current of the CV spectra (Fig. 5(a)). It is clear from Fig. 5(b) that with increasing cortisol concentration the current decreased linearly in the range 1 pM–100 nM, followed the linear equation ΔI (μA) = 21.85 + 1.63 log[cortisol conc. (M)], and exhibited a sensitivity of 1.63 μA M^{-1} with a correlation coefficient of 0.989. The results from multiple experiments (at least 3 sets), indicated by the error bars, revealed repeatability within 6%. For cortisol estimation, DPV studies were also carried out (Supplement Fig. 4). DPV studies showed that the cortisol can be detected in the 1 pM–100 nM range and followed ΔI (μA) = 32.59 + 2.39 log[cortisol conc. (M)]. The electrode exhibited a sensitivity of 2.39 μA M^{-1} and a correlation coefficient of 0.989.

3.3.4. *Interference studies*

Interference studies were conducted by testing the BSA/C-Mab/PPAuNP/Au electrodes for sequential incubation in PBS loaded with interferents for 30 min and testing through CV at 30 mV s^{-1}. The interferents used were BSA (10 μg ml^{-1}) and 17-α-OH-progesterone (100 nM) (Supplement Fig. 5). CV spectra (Supplement Fig. 5) showed the observed response of BSA/C-Mab/PPAuNP/Au electrodes towards interferents and cortisol (100 nM). A clear distinction of cortisol curve over BSA (a protein molecule) and 17-α-OH-progesterone (a similarly structured molecule from the cortisol family) suggests the specificity and selectivity of the electrode for cortisol estimation.

Table 1 shows the comparison of our electrode with other approaches used for cortisol estimation. From Table 1, it is clear that our system is simpler, better and can detect cortisol in wide range at neutral pH value, without requiring any external mediator.

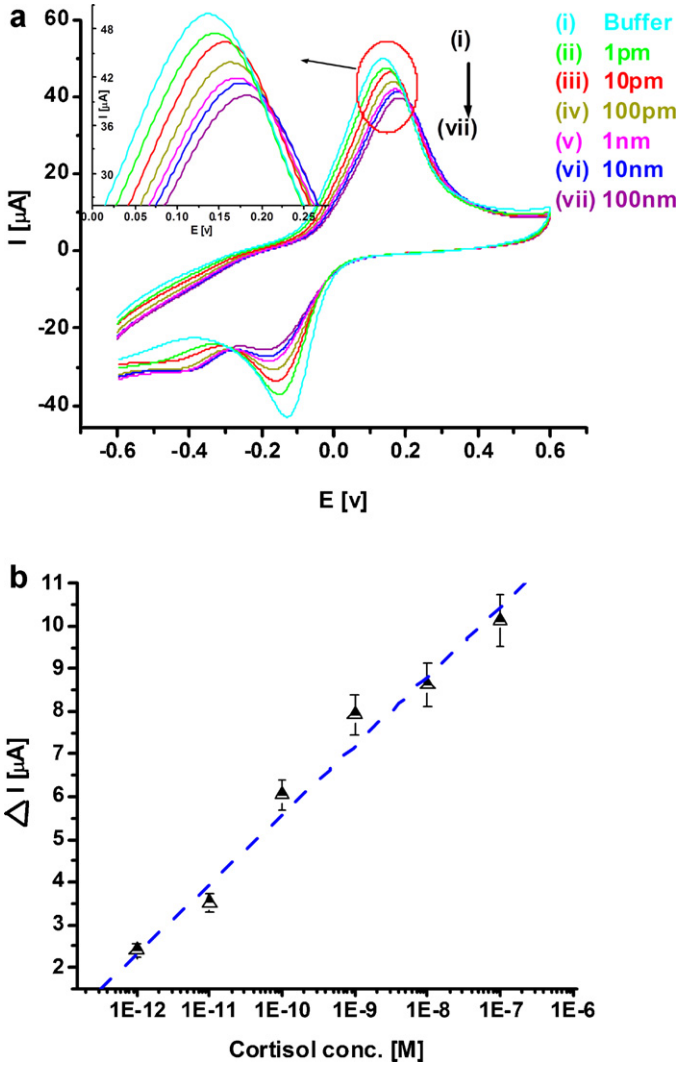

Fig. 5. (a) CV studies of BSA/C-Mab/PPAuNP/Au electrodes as a function of cortisol concentration: (i) buffer, (ii) 1 pM, (iii) 10 pM, (iv) 100 pM, (v) 1 nM, (vi) 10 nM and (vii) 100 nM. *Inset*: Zoomed image of the change in peak current with cortisol concentration. (b) Linearity curve for the peak current data obtained from CV studies for different cortisol concentrations.

4. Conclusions

A label and mediator free electrochemical biosensor based on polyaniline protected gold nanoparticles (PPAuNPs) has been fabricated for ultrasensitive cortisol estimation. PPAuNPs were synthesized in single step procedure, using aniline as the precursor and $HAuCl_4$ as the oxidant. For electrode fabrication, PPAuNPs were uniformly deposited onto a gold surface via electrophoretic deposition. The PPAuNP/Au electrode was modified with covalent binding of a cortisol antibody (C-Mab) and BSA blocking. CV studies revealed a stable peak for the fabricated electrode during repeated scanning, and well defined redox peaks in PBS solution of pH 7.0. The sensor was successfully tested for cortisol estimation in PBS without an external mediator or secondary labeling. CV results showed the cortisol detection up to 1 pM, with a sensitivity of 1.63 $\mu A\,M^{-1}$. The electrode was found to be selective against BSA and 17-α-OH progesterone and can be used for sensitive, mediator free estimation of cortisol.

Acknowledgement

SB would like to acknowledge the JSPS invitational fellowship program for support to work on the manuscript.

Appendix A. Supplementary data

Supplementary data associated with this article can be found, in the online version, at doi:10.1016/j.bios.2011.07.015.

References

Appel, D., Schmid, R., Dragan, C.-A., Bureik, M., Urlacher, V., 2005. Anal. Bioanal. Chem. 383 (2), 182–186.
Arya, S.K., Chornokur, G., Venugopal, M., Bhansali, S., 2010a. Analyst 135 (8), 1941–1946.
Arya, S.K., Chornokur, G., Venugopal, M., Bhansali, S., 2010b. Biosens. Bioelectron. 25 (10), 2296–2301.
Cook, N.J., Schaefer, A.L., Lepage, P., Morgan Jones, S.D., 1997. J. Agric. Food Chem. 45 (2), 395–399.
Dhand, C., Arya, S.K., Datta, M., Malhotra, B.D., 2008a. Anal. Biochem. 383 (2), 194–199.
Dhand, C., Arya, S.K., Singh, S.P., Singh, B.P., Datta, M., Malhotra, B.D., 2008b. Carbon 46 (13), 1727–1735.
Dhand, C., Das, M., Datta, M., Malhotra, B.D., 2011. Biosens. Bioelectron. 26 (6), 2811–2821.
Dhand, C., Malhotra, B.D., 2009. Organic Electronics in Sensors and Biotechnology. McGraw Hill, pp. 361–394.
Dhand, C., Singh, S.P., Arya, S.K., Datta, B., Malhotra, B.D., 2007. Anal. Chim. Acta 602, 244–251.
Feng, X., Mao, C., Yang, G., Hou, W., Zhu, J.J., 2006. Langmuir 22 (9), 4384–4389.
Feng, Y.Y., Yang, T., Zhang, W., Jiang, C., Jiao, K., 2008. Anal. Chim. Acta 616 (2), 144–151.
Gajendran, P., Saraswathi, R., 2008. Pure Appl. Chem. 80 (11), 2377–2395.
Gatti, R., Cappellin, E., Zecchin, B., Antonelli, G., Spinella, P., Mantero, F., De Palo, E.F., 2005. J. Chromatogr. B: Anal. Technol. Biomed. Life Sci. 824 (1–2), 51–56.
Hauer, D., Weis, F., Krauseneck, T., Vogeser, M., Schelling, G., Roozendaal, B., 2009. Brain Res. 1293, 114–120.
Kaptein, W.A., Zwaagstra, J.J., Venema, K., Ruiters, M.H.J., Korf, J., 1997. Sens. Actuators B 45 (1), 63–69.
Koh, W.C.A., Son, J.I., Choe, E.S., Shim, Y.B., 2010. Anal. Chem. 82 (24), 10075–10082.
Koutny, L.B., Schmalzing, D., Taylor, T.A., Fuchs, M., 1996. Anal. Chem. 68 (1), 18–22.
Kumar, A., Aravamudhan, S., Gordic, M., Bhansali, S., Mohapatra, S.S., 2007. Biosens. Bioelectron. 22 (9–10), 2138–2144.
Li, Y., Pang, X., Epand, R.F., Zhitomirsky, I., 2011. Mater. Lett. 65 (10), 1463–1465.
Liu, Y.G., Feng, X.M., Shen, J.M., Zhu, J.J., Hou, W.H., 2008. J. Phys. Chem. B 112 (30), 9237–9242.
Malhotra, B.D., Chaubey, A., Singh, S.P., 2006. Anal. Chim. Acta 578 (1), 59–74.
Mitchell, J.S., Lowe, T.E., Ingram, J.R., 2009. Analyst 134 (2), 380–386.
Murphy-Perez, E., Arya, S.K., Bhansali, S., 2011. Analyst 136, 1686–1689.
Njagi, J., Andreescu, S., 2007. Biosens. Bioelectron. 23, 168–175.
Oka, K., Noguchi, M., Kitamura, T., Shima, S., 1987. Clin. Chem. 33 (9), 1639–1642.
Ozdemir, C., Yeni, F., Odaci, D., Timur, S., 2010. Food Chem. 119 (1), 380–385.
Pandey, P., Singh, S.P., Arya, S.K., Gupta, V., Datta, M., Singh, S., Malhotra, B.D., 2007. Langmuir 23 (6), 3333–3337.
Petkus, M.M., McLauchlin, M., Vuppu, A.K., Rios, L., Garcia, A.A., Hayes, M.A., 2006. Anal. Chem. 78 (5), 1405–1411.
Rowe, L., Deo, S., Shofner, J., Ensor, M., Daunert, S., 2007. Bioconjugate Chem. 18 (6), 1772–1777.
Rui, Q., Komori, K., Tian, Y., Liu, H., Luo, Y., Sakai, Y., 2010. Anal. Chim. Acta 670 (1–2), 57–62.
Sarkar, M., Das, B.C., Bora, B.D., Kumar, V., Mohan, K., Meyer, H.H.D., Prakash, B.S., 2007. Gen. Comp. Endocrinol. 154, 85–90.
Schmalzing, D., Nashabeh, W., Yao, X.-W., Mhatre, R., Regnier, F.E., Afeyan, N.B., Fuchs, M., 1995. Anal. Chem. 67 (3), 606–612.
Shiigi, H., Morita, R., Yamamoto, Y., Tokonami, S., Nakao, H., Nagaoka, T., 2009. Chem. Commun. (24), 3615–3617.
Shiigi, H., Yamamoto, Y., Yoshi, N., Nakao, H., Nagaoka, T., 2006. Chem. Commun. (41), 4288–4290.
Shimomura, T., Itoh, T., Sumiya, T., Hanaoka, T.A., Mizukami, F., Ono, M., 2011. Sens. Actuators B 153 (2), 361–368.
Singh, R., Dhand, C., Sumana, G., Verma, R., Sood, S., Gupta, R.K., Malhotra, B.D., 2010. J. Mol. Recognit. 23 (5), 472–479.
Spain, E., Kojima, R., Kaner, R.B., Wallace, G.G., O'Grady, J., Lacey, K., Barry, T., Keyes, T.E., Forster, R.J., 2011. Biosens. Bioelectron. 26 (5), 2613–2618.
Stevens, R.C., Soelberg, S.D., Near, S., Furlong, C.E., 2008. Anal. Chem. 80 (17), 6747–6751.

Sun, K., Ramgir, N., Bhansali, S., 2008. Sens. Actuators B 133 (2), 533–537.
Sun, W., Zhai, Z., Wang, D., Liu, S., Jiao, K., 2009. Bioelectrochemistry 74 (2), 295–300.
Tai, S.S.C., Welch, M.J., 2004. Anal. Chem. 76 (4), 1008–1014.
Tian, S.J., Liu, J.Y., Zhu, T., Knoll, W., 2004. Chem. Mater. 16 (21), 4103–4108.
Wang, G.F., Huang, H., Zhang, G., Zhang, X.J., Fang, B., Wang, L., 2011. Langmuir 27 (3), 1224–1231.
Wang, J., 2006. Biosens. Bioelectron. 21 (10), 1887–1892.
Wang, Y., Liu, Z.M., Han, B.X., Sun, Z.Y., Huang, Y., Yang, G.Y., 2005. Langmuir 21 (3), 833–836.
Yang, W.R., Liu, J.Q., Zheng, R.K., Liu, Z.W., Dai, Y., Chen, G.N., Ringer, S., Braet, F., 2008. Nanoscale Res. Lett. 3 (11), 468–472.
Zhou, J.C., Chuang, M.H., Lan, E.H., Dunn, B., Gillman, P.L., Smith, S.M., 2004. J. Mater. Chem. 14 (14), 2311–2316.